ISSUE: August 2020

The Engineer's Guide To EMI In DC-DC Converters (Part 14): Behavioral Noise Modeling

by Timothy Hegarty, Texas Instruments, Phoenix, Ariz.

Electromagnetic interference (EMI) represents a major concern for power electronics system designers. As a result, predicting EMI has become an important aspect of any switching power-supply design. Parts 2 and 4 of this article series[1-13] reviewed noise propagation and filtering of conducted and radiated interference from dc-dc converters. More recently, parts 12 and 13 reviewed differential-mode (DM) and common-mode (CM) emissions, respectively, and simplified lumped-element models for noise prediction. The analysis considered the converter and its passive EMI filter stage as well as the measurement equipment, specifically the line impedance stabilization network (LISN) and EMI test receiver.

Even if many EMI prediction techniques are available, the most common method for studying EMI is to do so at the end of the design cycle, which entails measuring the EMI signature followed by the implementation of various techniques to reduce it. This often results in reduced power density and increased product costs.

Nevertheless, modeling is an advantageous way to evaluate system performance in the early stages of the design process. EMI modeling usually involves the characterization of noise sources and the essential coupling paths, and these models can be physics-based or behavioral models. Part 14 now provides an introduction to and overview of behavioral EMI models, where a compact association of noise sources and impedances identifies the dc-dc converter and its external EMI behavior.

This article will discuss two types of behavioral models—two-terminal (one-port), decoupling-mode models and three-terminal (two-port) models. Since the latter type of models provides greater accuracy, details on how to extract parameters for the three-terminal models will be presented. There are two methods for extracting these parameters and both will be described here. The article concludes by comparing DM and CM noise predictions obtained for a three-terminal model of a 50-W buck converter with bench measurements.

The Behavioral Modeling Approach

Existing models extracted to predict the EMI signature of dc-dc converter circuits can be classified into three main categories: lumped-element circuit models, decoupling-mode models and three-terminal models. Lumped-circuit models[2, 12-13] replace all semiconductor devices in the power stage with physics-based models and seek to include relevant parasitic elements of the circuit.

However, time-domain simulation of lumped-circuit models at EMI frequencies is quite complex and requires significant computational resources, often resulting in difficulties related to simulator convergence and long run times, and may lead to unusable results. The task is not easy even for a single standalone converter, and system-level EMI simulation (for example, with multiple converters powered from the same bus) is very challenging.

Behavioral modeling, a frequency-domain approach, overcomes these limitations and has proven to be quite promising even at frequencies up to 100 MHz. Both decoupling-mode models and three-terminal models are behavioral models offering different advantages and disadvantages with respect to simplicity and accuracy.

Decoupling-mode models use a two-terminal (or one-port) Thevenin- or Norton-equivalent circuit and model the DM and CM emissions separately. As an example, Fig. 1 shows a two-terminal model for DM noise where positive (P) and negative (N) terminals correspond to the input terminals of a boost converter. Using a Norton-equivalent circuit consisting of a noise current source and noise impedance, that circuit closely resembles the physical representation of the DM circuit described in part 2. One option to ensure well-defined source impedance is to use a standardized network such as a LISN connected at the input.

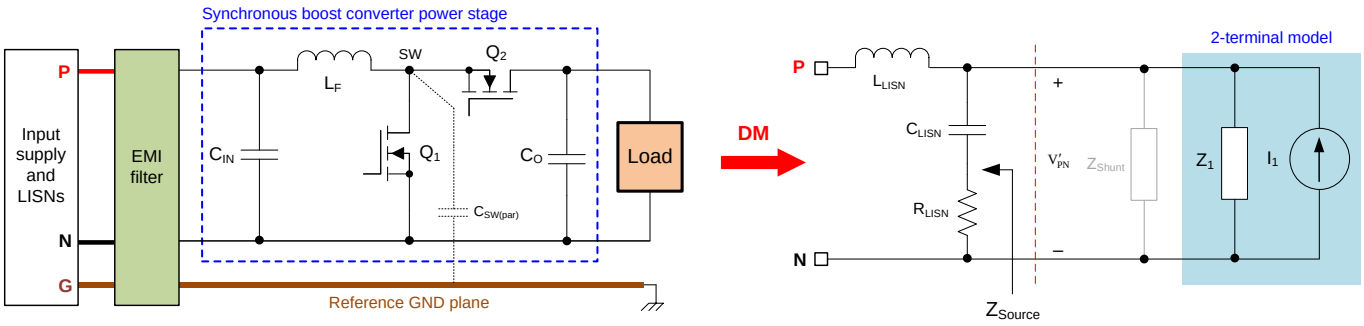

Fig. 1. The boost converter topology (a) and the associated two-terminal DM model (b), which is based on a Norton-equivalent circuit. A shunt impedance element (labeled Zshunt and typically a resistor and capacitor in series) is added to facilitate model parameter extraction.

Short- and open-circuit conditions typically define Norton-equivalent parameters, but these are not feasible test conditions with an operating converter. As an alternative, two distinct terminal-voltage measurements (V_{PN} and V'_{PN}) can identify the model parameters over the frequency range of interest. In addition to a nominal case, an appropriate RC shunt impedance (designated Z_{Shunt} in Fig. 1) establishes an attenuated case to facilitate a second measurement without affecting the circuit operating point. With an accurate knowledge of impedances Z_{Source} and Z_{Shunt} as well as the two measured terminal voltages V_{PN} and V'_{PN}, equation 1 explicitly solves for the equivalent circuit parameters, I_1 and Z_1:

$$\begin{aligned} V_{PN} &= I_1 \cdot Z_1 \| Z_{Source} \\ V'_{PN} &= I_1 \cdot Z_1 \| Z_{Source} \| Z_{Shunt} \end{aligned} \Rightarrow \begin{cases} I_1 = \dfrac{V_{PN} \cdot V'_{PN}}{Z_{Shunt} \cdot (V_{PN} - V'_{PN})} \\ Z_1 = \dfrac{Z_{Source} \cdot Z_{Shunt} \cdot (V_{PN} - V'_{PN})}{Z_{Source} \cdot V'_{PN} - Z_{Shunt} \cdot (V_{PN} - V'_{PN})} \end{cases} \quad (1)$$

where all quantities are denoted in the frequency domain.

A fast Fourier transform is a critical step in the modeling process, which facilitates the conversion of measured time-domain data to the frequency domain, and can be a significant source of error during model acquisition.[14] A mismatch at high frequency relates to the attenuation caused by the shunt impedance, and an important metric is the magnitude of difference between the two cases. Equation 2 rearranges equation 1 to express Z_1 and I_1 as a function of A:

$$A = \frac{V_{PN}}{V'_{PN}}, \quad Z_1 = \frac{(A-1) \cdot Z_{Source} \cdot Z_{Shunt}}{Z_{Source} - (A-1) \cdot Z_{Shunt}}, \quad I_1 = \frac{V_{PN}}{Z_{Shunt} \cdot (A-1)} \quad (2)$$

where A describes the change that Z_{Shunt} provides to the measured terminal voltage.

As A increases, the model approaches traditional open and short conditions for a Norton-equivalent circuit. Equation 3 summarizes the boundary conditions[15] to minimize the calculation error:

$$10 < A < 1000, \quad |Z_{Source}| > 0.1 \cdot |Z_1| \quad (3)$$

While one-port decoupling-mode models are considered simpler implementations than lumped-circuit models, limitations exist at high frequencies because of an incomplete treatment of mixed-mode noise when DM and CM

noise contributions cannot be accurately separated. In other words, neglecting mode transformation between DM and CM noises limits the accuracy of EMI predictions, especially for extended frequency modeling above 30 MHz.

Three-Terminal Behavioral Models

Generalized three-terminal (two-port) models capture the mixed-mode noise effect and can accurately predict conducted interferences generated by both filtered and unfiltered dc-dc converters. Several three-terminal models exist that differ by their performance, application and parameter extraction procedure.[14-18]

The simplest network that uniquely and fully defines a three-terminal system consists of two sources and three impedances. The impedances arrange in a delta configuration with an element connected between each terminal. Fig. 2 shows a generalized three-terminal Norton-equivalent circuit consisting of three impedances (Z_1 , Z_2 and Z_3) and two current sources (I_1 and I_2).

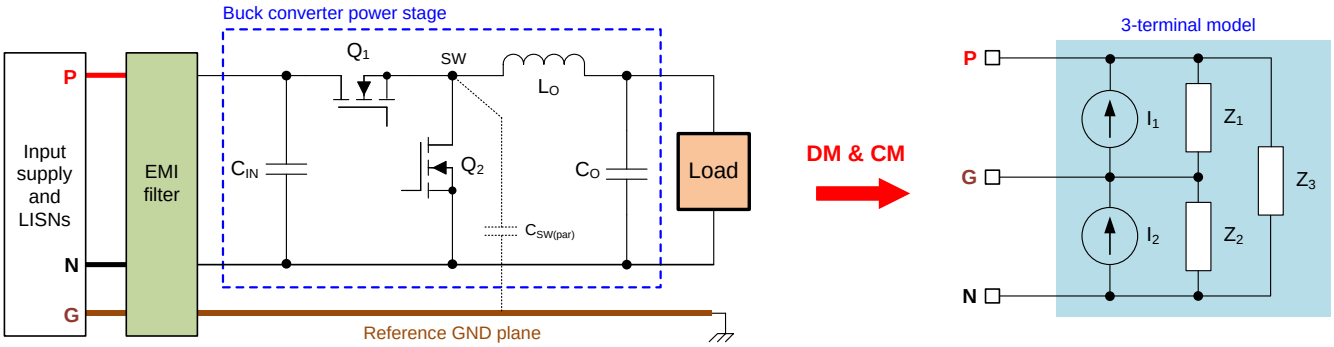

Fig. 2. A buck converter with switching-node parasitic capacitance included and powered through an EMI filter and LISNs (a) and its corresponding generalized, three-terminal model (b), which is based on a two-port Norton-equivalent circuit.

The three-terminal model in this example replaces the buck converter, where terminals designated positive (P), negative (N) and ground (G) match the corresponding input terminals of the buck converter. The system behaves essentially like a black box, as there is no a priori knowledge of its inner workings. Nevertheless, the model describes all essential coupling paths and circuit parameters and can deliver a full picture of EMI conduction and coupling mechanisms.

The basic inference from this discussion is that as long as the switching waveforms are not affected by insertion of the shunt impedance(s) (i.e. no change in the converter operating point) and the converter appears time-invariant at its input terminals, the terminal modeling method for approximating the EMI behavior of the power converter applies.

Identification Methods

Method No. 1: Attach Shunt Attenuator Impedances

Parameter identification for a three-terminal model requires a nominal case and at least two attenuated cases, as shown in Fig. 3. As before, an attenuated case exists when one or more shunt impedances inserted in the system significantly affect the voltages seen at the terminals.

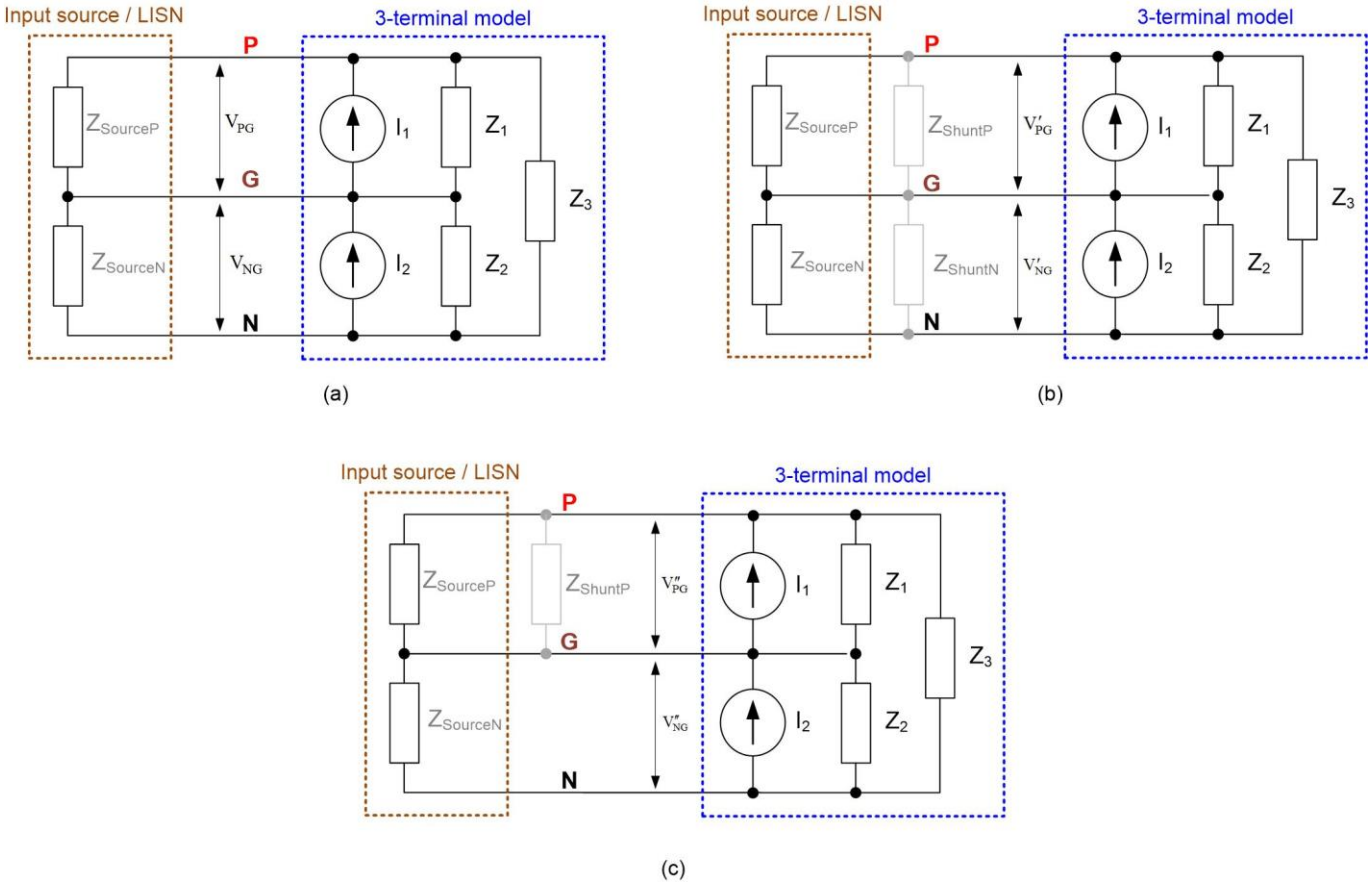

Fig. 3. Three-terminal model parameter extraction using a nominal case with no attenuation (a), an attenuated case with two impedances added (b), and an attenuated case with one impedance added (c). A LISN network provides a well-defined source impedance.

Seven different attenuation schemes are possible: three schemes with one impedance between any two terminals, three schemes with two impedances, or one scheme with three impedances in a delta configuration. Fig. 3b illustrates one of the schemes possible with two shunt impedances while Fig. 3c depicts one of the schemes possible with a single impedance.

Any two of these possibilities accompanied by a nominal system offer enough information to solve for the five unknown model parameters. Equation 4 provides expressions for the nominal case, and equation 5 offers corresponding expressions for two attenuated cases pictured in Fig. 3:

$$\begin{aligned} V_{PG} &= \left(I_1 - \frac{V_{PG} - V_{NG}}{Z_3} \right) \cdot Z_1 \| Z_{SourceP} \\ V_{NG} &= \left(-I_2 + \frac{V_{PG} - V_{NG}}{Z_3} \right) \cdot Z_2 \| Z_{SourceN} \end{aligned} \qquad (4)$$

$$\begin{aligned} V'_{PG} &= \left(I_1 - \frac{V'_{PG} - V'_{NG}}{Z_3} \right) \cdot Z_1 \| Z_{SourceP} \| Z_{ShuntP} \\ V'_{NG} &= \left(-I_2 + \frac{V'_{PG} - V'_{NG}}{Z_3} \right) \cdot Z_2 \| Z_{SourceN} \| Z_{ShuntN} \end{aligned}$$

$$\begin{aligned} V''_{PG} &= \left(I_1 - \frac{V''_{PG} - V''_{NG}}{Z_3} \right) \cdot Z_1 \| Z_{SourceP} \| Z_{ShuntP} \\ V''_{NG} &= \left(-I_2 + \frac{V''_{PG} - V''_{NG}}{Z_3} \right) \cdot Z_2 \| Z_{SourceN} \end{aligned} \qquad (5)$$

where the source impedances on the positive and negative lines are designated by $Z_{SourceP}$ and $Z_{SourceN}$, respectively, and the added common-mode (attenuator) impedances are Z_{ShuntP} and Z_{ShuntN}.

A total of eight different sets of two equations are possible, requiring a symbolic math solver or numerical solution. Equation 6 defines upper and lower bounds[15] on the attenuation and source impedances in order to minimize errors in the parameter extraction process:

$$\begin{cases} 20\text{dB} < A < 60\text{dB} \\ 0.1 \cdot |Z_1| < |Z_{SourceP}| < 10 \cdot |Z_1| \\ 0.1 \cdot |Z_2| < |Z_{SourceN}| < 10 \cdot |Z_2| \end{cases} \quad (6)$$

where A is the measured voltage attenuation provided by applicable shunt impedance, similar to that defined previously for the two-terminal model.

The extraction of a behavioral EMI terminal model for power converters with discontinuous input current (examples being buck and buck-boost converters) is more challenging given the presence of switched-impedance behavior at the input terminals. Taking a buck switching cell as an example, either infinite impedance or the load impedance appears at the input terminals, depending on the state of the high-side switch. Including an input capacitor provides a dominant impedance at the converter input terminals, thus masking the nonlinear part of the converter that has semiconductor switches and diodes.[17]

Method No. 2: Measure The Offline Input Impedances

A second technique, analytically developed based on estimating converter input impedances, requires only offline measurements, making the model easy to identify and applicable to high-power converters.[18] The converter is no longer treated as a black box during extraction of the noise source impedances, which facilitates the model parameter extraction process.

The model in Fig. 3 has three input impedances denoted by Z_{PG}, Z_{NG} and Z_{PN} as functions of Z_1, Z_2 and Z_3 in equation 7:

$$\begin{bmatrix} Z_{PG} \\ Z_{NG} \\ Z_{PN} \end{bmatrix} = \begin{bmatrix} \frac{Z_1 \cdot (Z_2 + Z_3)}{Z_1 + Z_2 + Z_3} \\ \frac{Z_2 \cdot (Z_1 + Z_3)}{Z_1 + Z_2 + Z_3} \\ \frac{Z_3 \cdot (Z_1 + Z_2)}{Z_1 + Z_2 + Z_3} \end{bmatrix} \quad (7)$$

Equation 8 solves the system of obtained equations for Z_1, Z_2 and Z_3 such that the model presents the same input impedances as the actual converter:

$$\begin{bmatrix} Z_1 \\ Z_2 \\ Z_3 \end{bmatrix} = \begin{bmatrix} \frac{Z_{PG}^2 + Z_{NG}^2 + Z_{PN}^2 - 2\left(Z_{PG}Z_{NG} + Z_{PG}Z_{PN} + Z_{NG}Z_{PN}\right)}{2\left(Z_{PG} - Z_{NG} - Z_{PN}\right)} \\ \frac{Z_{PG}^2 + Z_{NG}^2 + Z_{PN}^2 - 2\left(Z_{PG}Z_{NG} + Z_{PG}Z_{PN} + Z_{NG}Z_{PN}\right)}{2\left(-Z_{PG} + Z_{NG} - Z_{PN}\right)} \\ \frac{Z_{PG}^2 + Z_{NG}^2 + Z_{PN}^2 - 2\left(Z_{PG}Z_{NG} + Z_{PG}Z_{PN} + Z_{NG}Z_{PN}\right)}{2\left(-Z_{PG} - Z_{NG} + Z_{PN}\right)} \end{bmatrix} \quad (8)$$

It is possible to identify model current sources I_1 and I_2 using equation 9 as a function of voltages V_{PG} and V_{NG} and impedances Z_1, Z_2, Z_3 and $Z_{SourceP,N}$. Notice that the circuit is symmetrical, with no mixed-mode noise contribution if $Z_1 = Z_2$ and $Z_{SourceP} = Z_{SourceN}$:

$$\begin{bmatrix} I_1 \\ I_2 \end{bmatrix} = \begin{bmatrix} \frac{1}{Z_1} + \frac{1}{Z_3} + \frac{1}{Z_{SourceP}} & -\frac{1}{Z_3} \\ \frac{1}{Z_3} & -\left(\frac{1}{Z_2} + \frac{1}{Z_3} + \frac{1}{Z_{SourceN}}\right) \end{bmatrix} \begin{bmatrix} V_{PG} \\ V_{NG} \end{bmatrix} \quad (9)$$

If the converter has two switching states, equation 10 describes the three input impedances, Z_{PG}, Z_{NG} and Z_{PN},[19] as:

$$Z_{PG} = \frac{Z_{PG1} \cdot Z_{PG0}}{(1-D)Z_{PG1} + D \cdot Z_{PG0}}, \quad Z_{NG} = \frac{Z_{NG1} \cdot Z_{NG0}}{(1-D)Z_{NG1} + D \cdot Z_{NG0}}, \quad Z_{PG} = \frac{Z_{PN1} \cdot Z_{PN0}}{\left(1-D^2\right)Z_{PN1} + D^2 \cdot Z_{PN0}} \quad (10)$$

where suffixes 1 and 0 designate the applicable input impedances during each switching state, and D is the duty cycle.

The first step is to measure the six impedances Z_{PG1}, Z_{PG0}, Z_{NG1} Z_{NG0}, Z_{PN1} and Z_{PN0} using offline measurements with the converter unpowered (disconnected from the source) and placed over the ground plane in accordance with a typical EMI measurement setup. Taking a synchronous buck converter as an example, state 1 involves shorting the high-side switch to find Z_{PG1}, Z_{NG1} and Z_{PN1}, while state 0 requires shorting the low-side switch to allow the measurement of Z_{PG0}, Z_{NG0} and Z_{PN0}. Substituting each measured impedance into the appropriate expression in equation 10 subsequently identifies model impedances Z_1, Z_2 and Z_3 using equation 8, and model sources I_1 and I_2 using equation 9.

Practical Measurements

Fig. 4 shows plots of identified model parameters in the frequency band from 100 kHz to 108 MHz.[18] The buck converter operates on a laboratory test bench in accordance with the CISPR 25 standard. Fig. 5 compares the conducted emissions through system measurement and three-terminal model prediction, indicating close agreement.

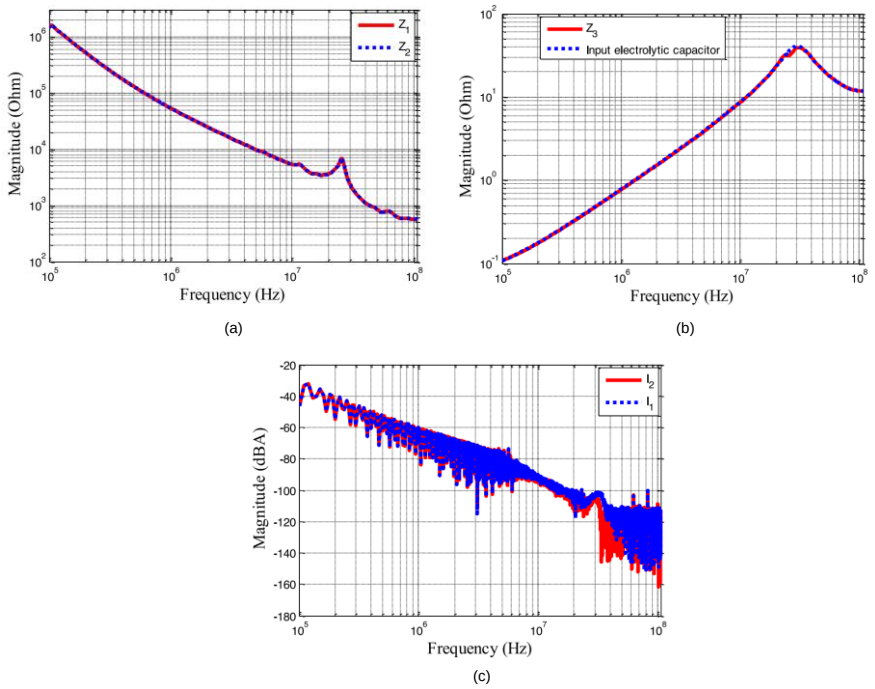

Fig. 4. Plots of model impedances Z_1 and Z_2 (a), model impedance Z_3 (b), and current sources I_1 and I_2 versus frequency (c).

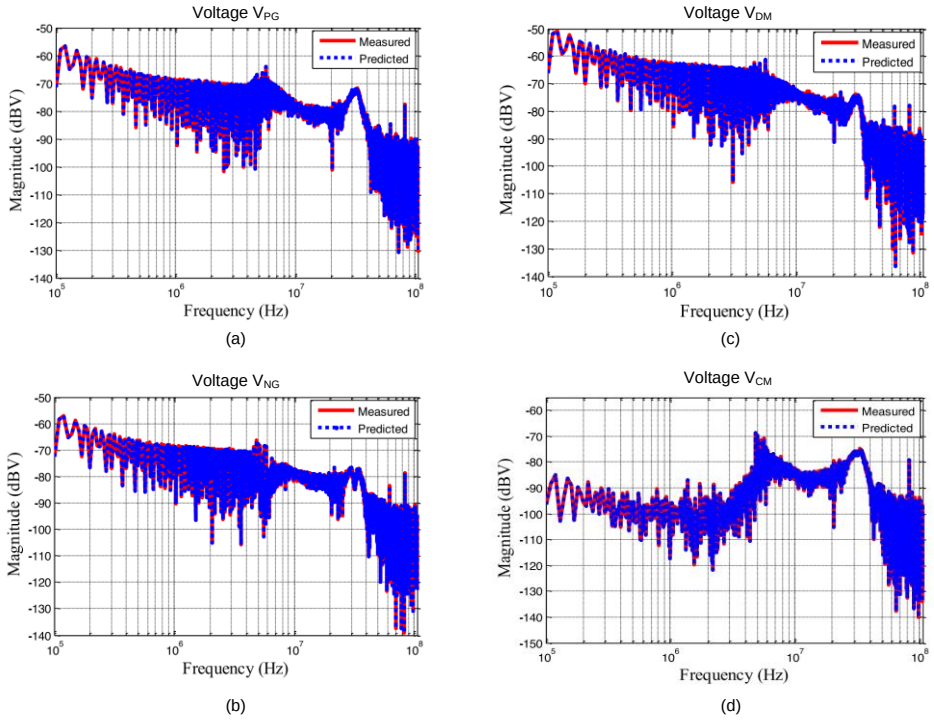

Fig. 5. Comparison of conducted emissions through system measurement and three-terminal model prediction for a 50-W buck converter: positive LISN voltage (a), negative LISN voltage (b), DM voltage (c), and CM voltage (d).

Summary

Measurement-based, three-terminal behavioral EMI models can effectively capture the EMI signature of switched power converters. Such models run in the frequency domain and are compact and linear, enabling faster and more stable simulations compared to lumped-circuit models.

Under the condition that the load side of the converter remains fixed, these "terminated" models can predict input-side EMI for any impedance change of the input-side network. Since these models are reduced order with only a few sources and impedances, they simulate without any significant convergence problems.

With a complete model realized with noise sources and impedances, interactions between systems and filters enable the prediction of EMI and filter design. I recommend reviewing references 14 to 18 for an in-depth treatment on the subject.

References

1. "The Engineer's Guide To EMI In DC-DC Converters (Part 1): Standards Requirements And Measurement Techniques," by Timothy Hegarty, How2Power Today, December 2017 issue.
2. "The Engineer's Guide To EMI In DC-DC Converters (Part 2): Noise Propagation And Filtering," by Timothy Hegarty, How2Power Today, January 2018 issue.
3. "The Engineer's Guide To EMI In DC-DC Converters (Part 3): Understanding Power Stage Parasitics," by Timothy Hegarty, How2Power Today, March 2018 issue.
4. "The Engineer's Guide To EMI in DC-DC Converters (Part 4): Radiated Emissions," by Timothy Hegarty, How2Power Today, April 2018 issue.
5. "The Engineer's Guide To EMI In DC-DC Converters (Part 5): Mitigation Techniques Using Integrated FET Designs," by Timothy Hegarty, How2Power Today, June 2018 issue.
6. "The Engineer's Guide To EMI In DC-DC Converters (Part 6): Mitigation Techniques Using Discrete FET Designs," by Timothy Hegarty, How2Power Today, September 2018 issue.
7. "The Engineer's Guide To EMI In DC-DC Converters (Part 7): Common-Mode Noise Of A Flyback," by Timothy Hegarty, How2Power Today, December 2018 issue.
8. "The Engineer's Guide To EMI In DC-DC Converters (Part 8): Common-Mode Noise Mitigation In Isolated Designs," by Timothy Hegarty, How2Power Today, February 2019 issue.
9. "The Engineer's Guide To EMI In DC-DC Converters (Part 9): Spread-Spectrum Modulation," by Timothy Hegarty, How2Power Today, August 2019 issue.
10. "The Engineer's Guide To EMI In DC-DC Converters (Part 10): Input Filter Impact On Stability," by Timothy Hegarty, How2Power Today, November 2019 issue.
11. "The Engineer's Guide To EMI In DC-DC Converters (Part 11): Input Filter Impact On Dynamic Performance," by Timothy Hegarty, How2Power Today, January 2020 issue.
12. "The Engineer's Guide To EMI In DC-DC Converters (Part 12): Predicting The Differential-Mode Conducted Noise Spectrum," by Timothy Hegarty, How2Power Today, April 2020 issue.
13. "The Engineer's Guide To EMI In DC-DC Converters (Part 13): Predicting The Common-Mode Conducted Noise Spectrum," by Timothy Hegarty, How2Power Today, June 2020 issue.
14. "Generalized terminal modeling of electromagnetic interference" by Andrew Baisden et al., IEEE Transactions on Industry Applications 46, No. 5 (September-October 2010): 2068-2079.

15. "'Black box' EMC model for power electronics converter" by Mikael Foissac et al., IEEE Energy Conversion Congress and Exposition (September 2009): 3609-3615.

16. "Analysis of EMI terminal modeling of switched power converters" by Hemant Bishnoi et al., IEEE Transactions on Power Electronics 27, No. 9 (September 2012): 3924-3933.

17. "EMI modeling of buck converter using a generalized terminal model" by Hemant Bishnoi et al., Proceedings of the Society for Modeling and Simulation International (SCS), Grand Challenges in Modeling and Simulations (GCMS) (July 2010): 158-164.

18. "New EMI model with the same input impedances as converter" by Bouzid Kerrouche et al., IEEE Transactions on Electromagnetic Compatibility 61, No. 4 (August 2019): 1072-1081.

About The Author

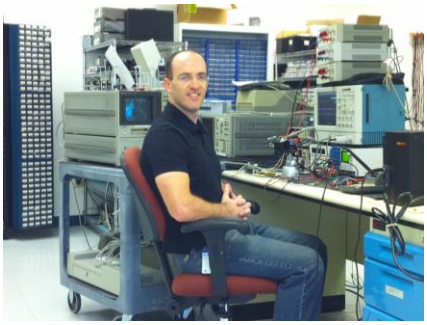

Timothy Hegarty is an applications engineer for the Buck Switching Regulators business unit at Texas Instruments. With over 23 years of power management engineering experience, he has written numerous conference papers, articles, seminars, white papers, application notes and blogs.

Tim's current focus is on enabling technologies for high-frequency, low-EMI, isolated and nonisolated regulators with wide input voltage range, targeting industrial, communications and automotive applications in particular. He is a senior member of the IEEE and a member of the IEEE Power Electronics, Industrial Applications and EMC Societies.

For more information on EMI, see How2Power's Power Supply EMI Anthology. Also see the How2Power's Design Guide, locate the Design Area category and select "EMI and EMC".